



**Dynamics of the Earth-Moon-Sun System and
How It Impacts the Solar Wind Implanted
Hydrogen Distribution on the Moon**

Michael J. Zalewski

**October 1999
(Revised January 2000)**

UWFDM-1109

***FUSION TECHNOLOGY INSTITUTE
UNIVERSITY OF WISCONSIN
MADISON WISCONSIN***

**Dynamics of the Earth-Moon-Sun System and How It
Impacts the Solar Wind Implanted Hydrogen
Distribution on the Moon**

Michael J. Zalewski

Fusion Technology Institute
Department of Engineering Physics
University of Wisconsin-Madison
1500 Engineering Drive
Madison, WI 53706

October 1999
Revised January 2000

UWFDM-1109

Progress Report to the National Space Society Center for Lunar Research Summer Internship

Abstract

Recent neutron spectrometer measurements by the Lunar Prospector Mission indicate the presence of unexpectedly high concentrations of hydrogen, possibly due to water ice, at the polar regions of the Moon. The objective of the conducted research was to analyze the solar-wind-implanted hydrogen on the Moon in order to interpret the Lunar Prospector results. Previous researchers had created a helium distribution map by utilizing the simple assumptions of purely radial flow of the solar wind, an untilted Moon, and shielding of the Moon by the Earth's magnetosphere during 25% of the lunar orbit. The present research refines that analysis to include the small tilt of the lunar axis to the ecliptic plane and arbitrary magnetospheric shielding. It also formulates the problem to include arbitrary x, y, and z components of the solar wind velocity, although the resulting equations are not solved here.

1. Introduction

Potentially valuable hydrogen and helium resources, deposited by the solar wind, exist on the lunar surface. In particular, Lunar Prospector observed lunar hydrogen [1, 2], which may indicate water ice, and the rare isotope helium-3 has been identified as an important resource for terrestrial fusion power [3, 4]. The present research analyzes the deposition of the solar wind hydrogen and helium on the lunar surface. Previously, this problem had been analyzed only for helium-3 with the fairly simple assumptions of purely radial flow of the solar wind from the Sun, an untilted Moon, and complete shielding by the Earth's magnetosphere for 25% of the Moon's orbit [5, 6]. Accurate assessment of the solar wind implantation requires a more sophisticated model, however, because of the small tilt ($1^{\circ}32'$) of the lunar axis off the ecliptic plane, the small z -component of the solar wind velocity, and variable shielding by the magnetosphere. The tilt and z -component effects are particularly important for the solar wind implantation near the lunar poles. The present calculations extend the earlier work by including the effects of the tilt of the lunar axis and a more general shielding by the magnetosphere. The non-ecliptic component of the solar wind velocity can be treated by using the same mathematical formalism as for the lunar axis tilt and integrating over a distribution function for the solar wind velocity. The present research sets up the formalism for using a model distribution function for the solar wind velocity, although developing it is beyond the present scope.

The solar wind in the vicinity of Earth flows in a mainly radial direction from the Sun and strikes the Moon with an average speed of about 400 km/s. The instantaneous solar wind speed, however, deviates considerably from this average, ranging from approximately 200–700 km/s and includes non-radial components. The magnitude and direction of the solar wind's velocity at the Moon are influenced by many complex processes, including the Sun's surface conditions, solar radiation interacting with the ions in flight, plasma instabilities, and the Earth's magnetosphere. The problem of the shielding of the Moon from the solar wind by the Earth's magnetosphere involves calculating the diffusion of ions into the magnetosphere by both collisions and plasma instabilities, plus assessing the interaction of the Moon with the solar wind flowing around the magnetosphere and with the plasma in the magnetotail. Although researchers are making good progress in understanding these processes, that research remains at an early stage and is beyond the scope of the present project. The magnetospheric shielding, therefore, is treated in a simplified way by assuming complete shielding of the Moon by the magnetosphere for a parameterized fraction of the lunar orbit. Because this shielding, even if complete, affects less than 25% of the lunar orbit, this approximation should not dramatically alter the results.

The complicated dynamics of lunar motion in the Earth-Moon-Sun system are simplified here by assuming planar, circular orbits and uniform orbital speed. The technical approach to the problem of a tilted Moon or solar wind components off the ecliptic plane is to use Euler angles to transform from lunar latitude and longitude to a tilted coordinate system that rotates separately with lunar month and year angular velocities. The boundary conditions for solar illumination of the Moon and shielding by the magnetosphere can then be implemented with relative simplicity.

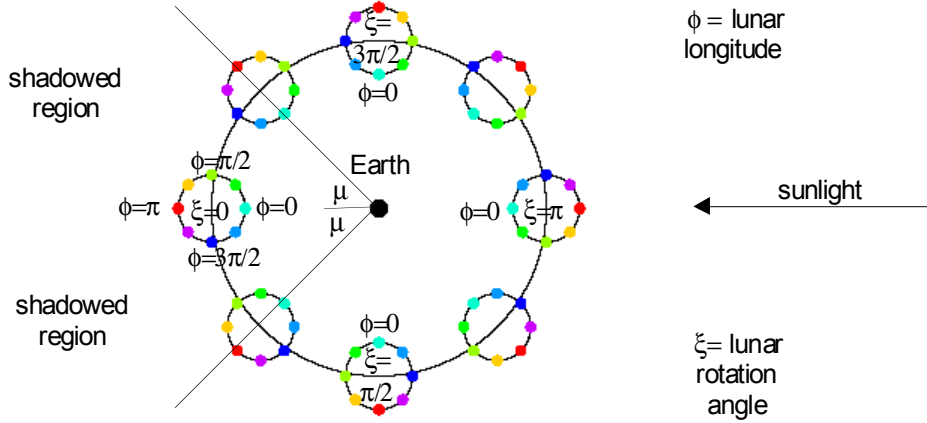


Figure 1. Lunar orbit and magnetospheric shielding.

2. Untilted Moon

Two effects are responsible for the variation in solar-wind deposition with respect to lunar latitude and longitude. The first effect is strictly geometrical in that the deposition is equal to the cosine of the latitude. The second effect is due to both geometry (cosine of longitude) and solar wind shielding by the Earth's magnetosphere. The assumption here is that the moon is completely shielded for 2μ of its orbit around the Earth.

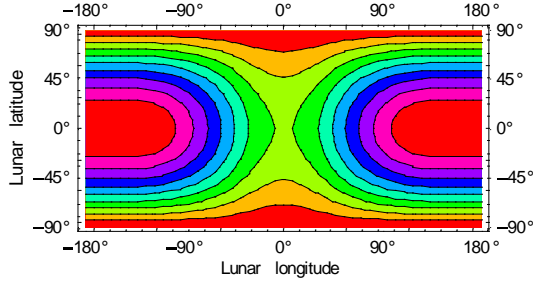
Figure 1 illustrates the model used for the motion of the Moon around the Earth and the range during which magnetospheric shielding occurs. Each colored point on the Moon in Figure 1 represents an example longitude. The movement of each point can be seen by following the orbit of the Moon around the Earth. The figure not only served as a visual aid for understanding the dynamic system, but it also helped develop the necessary boundary conditions for the deposition equations.

Points that are not illuminated by the solar wind satisfy $\frac{\pi}{2} \leq \phi + \xi \leq \frac{3\pi}{2} \pmod{2\pi}$. Shielding of the Moon from the solar wind by the Earth's magnetosphere occurs when $-\mu \leq \xi \leq \mu$. Without magnetospheric shielding, the instantaneous solar wind flux, $f(\theta, \phi)$, at a point on the Moon is given by the projection of the solar wind onto the spherical lunar surface:

$$\begin{aligned}
 f(\theta, \phi) &\equiv \Gamma_0 \cos \theta \cos(\phi + \xi) & \text{for } 0 \leq \phi + \xi \leq \frac{\pi}{2} \\
 &\equiv 0 & \text{for } \frac{\pi}{2} \leq \phi + \xi \leq \frac{3\pi}{2} \\
 &\equiv \Gamma_0 \cos \theta \cos(\phi + \xi) & \text{for } \frac{3\pi}{2} \leq \phi + \xi \leq 2\pi,
 \end{aligned}$$

where θ is the lunar latitude, ϕ is the longitude, ξ is the lunar rotation angle around the Earth, and Γ_0 is a suitable normalization constant. The zero of longitude ($\phi=0$) is defined here to be the sub-Earth

a) $\mu = \pi/4$



b) $\mu = \pi/7$

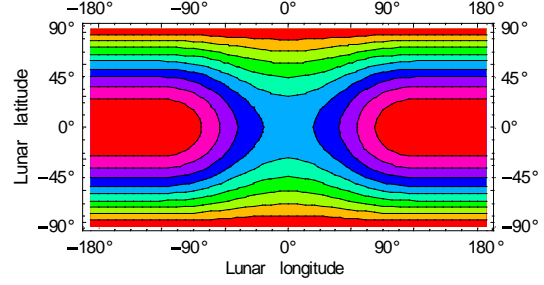


Figure 2. Solar wind initial deposition contours: a) $\mu = \pi/4$, b) $\mu = \pi/7$.

point (always faces toward the Earth). The total solar wind fluence (time-integrated flux) over one lunar rotation is thus:

$$\Gamma(\theta, \phi) = \int_{\mu}^{2\pi - \mu} d\xi f(\theta, \phi).$$

In using this equation to generate maps of the solar-wind deposition, the assumption is made that the solar wind has been constant over the time of deposition ($>10^9$ years), so that the single-rotation value reasonably approximates the time-averaged fluence. Substituting for f in the fluence integral yields the following deposition equations:

$$\begin{aligned} \Gamma(\theta, \phi) &= \Gamma_0 \cos \theta [\sin(\phi - \mu) - \sin(\phi + \mu)] && \text{for } -\mu < \phi < \mu \\ &= \Gamma_0 \cos \theta [1 + \sin(\phi - \mu)] && \text{for } \mu < \phi < \pi - \mu \\ &= 2 \Gamma_0 \cos \theta && \text{for } \pi - \mu < \phi < \pi + \mu \\ &= \Gamma_0 \cos \theta [1 - \sin(\phi - 2\pi + \mu)] && \text{for } \pi + \mu < \phi < 2\pi - \mu. \end{aligned}$$

From the deposition equations, it is clear that there is a difference in hydrogen distribution with latitude and longitude between the near and far side of the Moon. The resulting solar wind distribution maps for the cases $\mu = \pi/4$ and $\mu = \pi/7$ are shown in Figure 2. The $\pi/7$ case corresponds to four days, which has been used by some researchers for the magnetospheric shielding time [7]. Figure 2a agrees well with earlier figures in Refs. 5 and 6. When the deposition equations of Ref. 6 are corrected for an apparent typographical error, our formulas agree exactly.

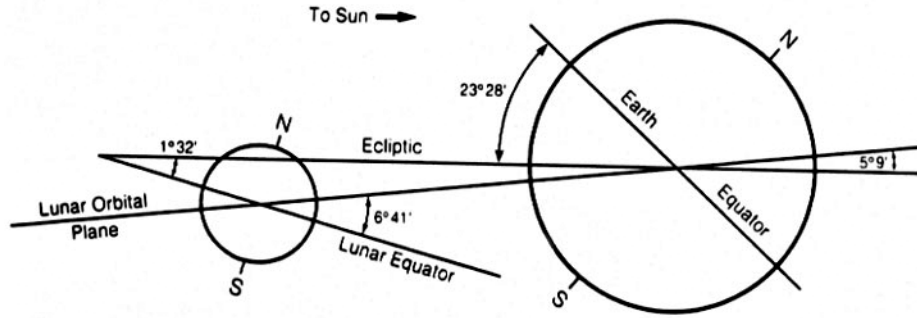


Figure 3. Earth-Moon-Sun system orbital planes and spin-axis tilt angles [8].

3. Tilted Moon

The research conducted expands on the previous model in three ways:

1. It allows an arbitrary tilt of the lunar axis off the ecliptic plane.
2. It sets up the closely related problem of arbitrary directions for the solar-wind velocity.
3. Magnetospheric shielding of the Moon can be for any fraction of the lunar orbit.

The lunar spin axis is tilted only $1^{\circ}32'$ to the ecliptic plane (see Figure 3) and the non-ecliptic component of the solar wind velocity generally remains within 10° of the ecliptic, so these effects make a significant difference only near the lunar poles. Nevertheless, magnetospheric shielding of a moon by its planet is a common situation in the solar system and the lunar poles are potentially important, so we have chosen to set up the equations for the general problem.

3.1 Inclusion of the Moon's Rotations and Axis Tilt

To factor in the Moon's rotations and small axial tilt into the model, Euler angles can be employed. The three Euler angles used are ζ , ψ , and ξ , with ζ being the angle in the Moon's orbit around the Earth, ψ being the lunar axis tilt angle, and ξ being the angle in the Earth's (and Moon's) orbit around the Sun. The angles ζ and ξ must be treated separately, because ζ controls magnetospheric shielding of the Moon, while ξ controls the precession of the lunar axis with respect to the Sun. The spherical coordinates of a point $\{R_m, \theta, \phi\}$ on the lunar surface, where the lunar radius (R_m) is assumed constant, are first converted to Cartesian coordinates. The Euler rotation matrix, \mathfrak{R} , which is $\mathfrak{R}(-\xi-\pi/2, \psi, \zeta+\pi/2)$ for our conventions, is given by

$$\mathfrak{R} = \begin{bmatrix} \cos \zeta \cos \xi \cos \psi + \sin \zeta \sin \xi & \cos \xi \sin \zeta - \cos \psi \cos \zeta \sin \xi & \cos \zeta \sin \psi \\ \cos \zeta \sin \xi - \cos \xi \cos \psi \sin \zeta & \sin \zeta \sin \xi \cos \psi + \cos \zeta \cos \xi & -\sin \zeta \sin \psi \\ -\cos \xi \sin \psi & \sin \xi \sin \psi & \cos \psi \end{bmatrix}$$

It rotates the Cartesian coordinates into primed Cartesian coordinates, where they are transformed to primed spherical coordinates, $\{R_m, \theta', \phi'\}$. The resulting equations are:

$$\theta' = \cos^{-1} \left[\frac{(\cos \theta \cos \psi - \cos \xi \cos \phi \sin \theta \sin \psi + \sin \theta \sin \xi \sin \phi \sin \psi)}{\left((\cos \phi \sin \theta (\cos \zeta \cos \xi \cos \psi + \sin \zeta \sin \xi) + \sin \theta (\cos \xi \sin \zeta - \cos \zeta \cos \psi \sin \xi)) \sin \phi + \cos \zeta \cos \theta \sin \psi \right)^2 + (\cos \phi \sin \theta (\cos \zeta \sin \xi - \cos \xi \cos \psi \sin \zeta) + \sin \theta (\cos \zeta \cos \xi + \cos \psi \sin \zeta \sin \xi)) \sin \phi - \cos \theta \sin \zeta \sin \psi \right)^2 + (\cos \theta \cos \psi - \cos \xi \cos \phi \sin \theta \sin \psi + \sin \theta \sin \xi \sin \phi \sin \psi)^2} \right]$$

$$\phi' = \tan^{-1} \left[\frac{\cos \phi \sin \theta (\cos \zeta \cos \xi \cos \psi + \sin \zeta \sin \xi) + \sin \theta (\cos \xi \sin \zeta - \cos \zeta \cos \psi \sin \xi) \sin \phi + \cos \zeta \cos \theta \sin \psi}{\cos \phi \sin \theta (\cos \zeta \sin \xi - \cos \xi \cos \psi \sin \zeta) + \sin \theta (\cos \zeta \cos \xi + \cos \psi \sin \zeta \sin \xi) \sin \phi - \cos \theta \sin \zeta \sin \psi} \right]$$

Mathematically, these transformations present a problem at the poles of the primed spherical coordinate system because of the degeneracy of the ϕ' (longitude) coordinate there. Physically, of course, no problem exists, because the transformation is unique. Therefore, we arbitrarily choose $\phi'=0$ for the primed polar points. The primed polar values and their corresponding unprimed points are

$$\begin{aligned} \theta' = 0, \quad \phi' = 0 & \quad \text{for } \psi = \theta, \quad \xi = \pi - \phi \\ \theta' = \pi, \quad \phi' = 0 & \quad \text{for } \psi = \pi - \theta, \quad \xi = -\phi. \end{aligned}$$

A further mathematical problem exists because Mathematica uses a form of the arctan function that does not cancel a $\sin \psi$ that appears in both numerator and denominator, thereby causing difficulties for $\sin \psi=0$. For this case, we have chosen to use a ϕ' solution consistent with a point infinitesimally off the pole:

$$\begin{aligned} \theta' = 0, \quad \phi' = \phi + \xi - \zeta & \quad \text{for } \psi = 0 \\ \theta' = \pi, \quad \phi' = \pi - \phi + \xi - \zeta & \quad \text{for } \psi = \pi. \end{aligned}$$

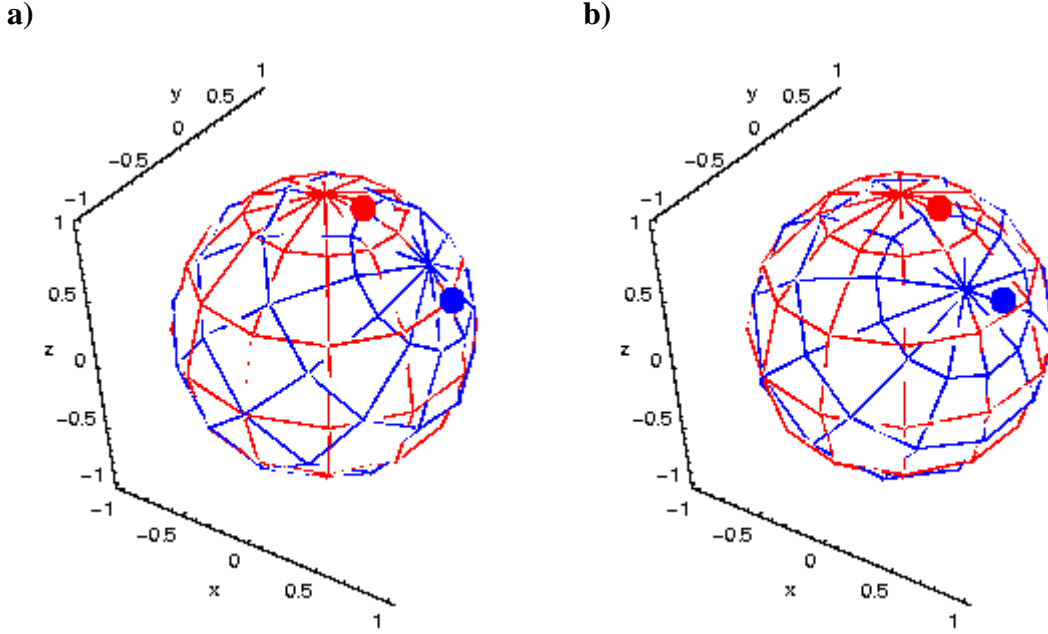


Figure 4. Tests of coordinate transformation. Red=unprimed coordinates; Blue=primed coordinates.
a) $\psi=\pi/4, \xi=0, \zeta=0$. b) $\psi=\pi/4, \xi=\pi/3, \zeta=\pi/6$.

Figure 4 illustrates two of several cases that were used to check the transformation. Because the primed spherical coordinates are referenced to the Sun, with the line $\phi'=0$ designated to be the sub-Sun point, the illuminated and dark sides of the Moon can easily be separated in these coordinates.

The instantaneous solar-wind deposition function, referenced to the primed coordinates, is simply the projection of the essentially planar solar wind onto a sphere:

$$\Gamma(\theta, \phi, \xi, \psi, \zeta) \equiv \Gamma_0 \cos \theta' \cos \phi' = \Gamma_0 \cos[\theta'(\theta, \phi, \xi, \psi, \zeta)] \cos \phi'(\theta, \phi, \xi, \psi, \zeta)$$

with θ' and ϕ' given above and Γ_0 a normalization constant.

For a given tilt-angle ψ and $\{\theta, \phi\}$ point on the lunar surface, the deposition function must be integrated over the monthly and yearly lunar rotations. In the primed coordinate system, the magnetospheric shielding takes the simple form

$$\begin{aligned} \Gamma(\theta, \phi, \xi, \psi, \zeta) &\equiv \Gamma_0 \cos \theta' \cos \phi' && \text{for } 0 \leq \phi' \leq \frac{\pi}{2} \\ &\equiv 0 && \text{for } \frac{\pi}{2} \leq \phi' \leq \frac{3\pi}{2} \\ &\equiv \Gamma_0 \cos \theta' \cos \phi' && \text{for } \frac{3\pi}{2} \leq \phi' \leq 2\pi. \end{aligned}$$

The total time-averaged deposition at a point on the lunar surface is thus

$$\Phi(\theta, \phi, \psi) \equiv \int_{\mu}^{2\pi-\mu} \int_0^{2\pi} \Gamma(\theta, \phi, \xi, \psi, \zeta) d\zeta d\xi.$$

3.2 Addition of the Z-Component of Solar-Wind Velocity

The solar-wind velocity is not just in the radial direction but usually has a small component in the z -direction, as shown in Figure 5. A good recent source for relevant data is the solar wind experiment (SWE) aboard the WIND spacecraft [9]. Its data is available at the National Space Science and Data Center web site: <http://nssdc.gsfc.nasa.gov/space/netdex.html>.

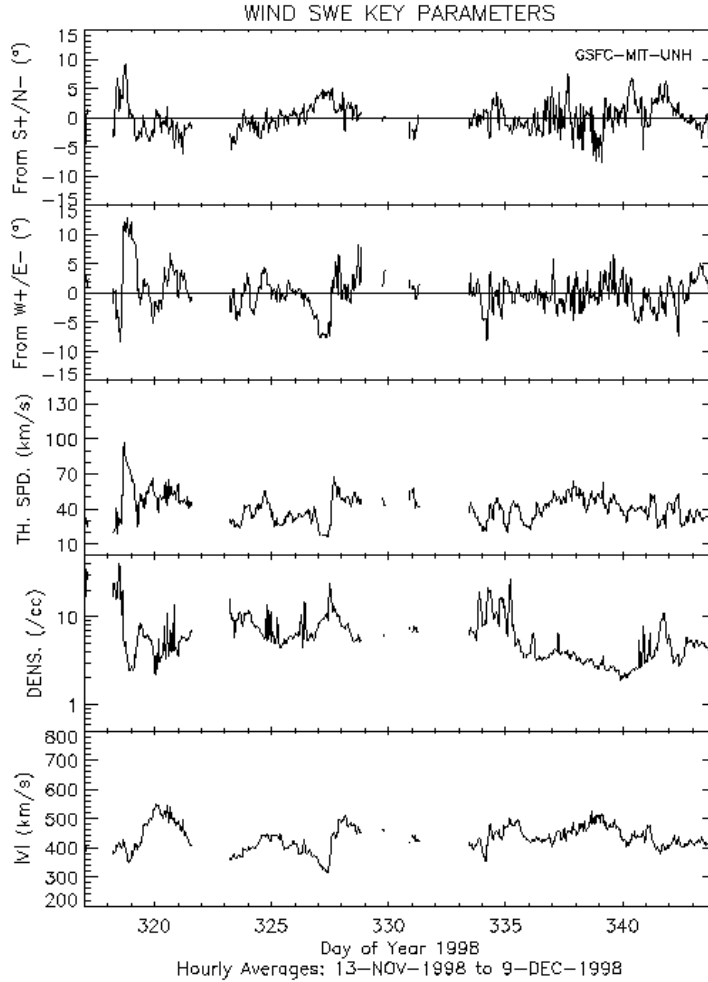


Figure 5. Key plasma ion velocity parameters measured by the WIND solar-wind experiment (SWE) [9].

Including the z -component of the solar-wind velocity into the model is very similar to including the lunar axis tilt, ψ_{tilt} . By knowing the angle of incidence that the solar wind makes with the lunar poles, the “effective” tilt can be calculated. For an instantaneous angle ψ_{sw} of the solar wind’s velocity off the z axis (normal to the ecliptic), the effective tilt angle is $\psi_{\text{eff}} = \psi_{\text{tilt}} - \psi_{\text{sw}}$. Averaging over an appropriate distribution function for the solar-wind velocity components would give a refined distribution of the initially implanted solar-wind hydrogen and helium on the Moon. Mathematically, the required modification to the calculation of $\Phi(\theta, \phi, \psi)$ is to multiply $\Gamma(\theta, \phi, \xi, \psi, \zeta)$ in the integrand by a suitable solar-wind distribution function:

$$f[\theta'(\theta, \phi, \xi, \psi, \zeta), \phi'(\theta, \phi, \xi, \psi, \zeta)],$$

where it has been assumed that the distribution function will be written most conveniently in terms of the $\{\theta', \phi'\}$ variables.

4. Future Work

The required transformations have been carried out, and the problem set up to calculate the initial solar-wind deposition on the Moon. Problems arose in performing the numerical integration, most likely due to our implementation of the functions and integral in the Mathematica computer program, and these were not resolved in time to be included in this Progress Report. They will be included in a future publication [10].

A valuable addition to the present research would be the development of long-time-averaged ion velocity distribution functions, including the non-ecliptic component, for the solar wind. The formalism developed here could then be applied to including this effect, which could have a significant impact on the solar-wind volatile inventory near the lunar poles.

The deposition contours resulting from carrying out the above analyses should be compared to observations. This will require making assumptions for the relative trapping of solar-wind volatiles in various minerals plus correlating suitably with factors such as regolith maturity—as recently done, for example, by Johnson, et al. [6] for helium-3 in the untilted-Moon case. Rates of diffusion of volatiles from the regolith into the lunar atmosphere will also have a significant effect on their inventories. Such calculations would be helpful in interpreting the corresponding results from the Lunar Prospector and other missions.

The result of the previously discussed steps would be a detailed map of the initial implantation of solar-wind hydrogen and helium in the lunar regolith. The next step would be to investigate the subsequent diffusion of the volatiles into the lunar atmosphere, their ionization, pickup by the solar-wind’s magnetic field, and subsequent loss into space or redeposition on the Moon. The research would be extremely useful for locating resources of hydrogen, helium-3, and other lunar volatiles. A preliminary analysis of the lunar pickup-ion problem has been performed in a related NSS summer internship project [11, 12].

5. Conclusions

A formalism has been created for the general problem of solar-wind deposition on a rotating moon with its axis tilted at an arbitrary angle to the ecliptic plane and complete magnetospheric shielding for an arbitrary fraction of the moon's orbit. This formalism has been applied to the Earth-Moon-Sun system. The coordinate-system transformations and techniques for handling the related mathematical degeneracies have been exhibited. The untilted lunar axis problem has been solved for arbitrary magnetospheric shielding and found to agree with a previously published result at 25% shielding. The final numerical integration to calculate the deposition values for the tilted lunar axis problem has not yet been completed. Including the lunar-axis tilt and non-ecliptic component of the solar wind is anticipated to have a significant effect on the volatile inventory near the lunar poles.

Acknowledgements

The author thanks Dr. John F. Santarius for guidance on this project, as well as the support of Dr. Gerald Kulcinski and Dr. Harrison Schmitt. Thanks to the University of Wisconsin Fusion Technology Institute and the National Space Society's Center for Lunar Research for the funding to make this research possible. Many of the calculations were performed using Mathematica 3.0 on a Windows NT 4.0 PC.

References

1. Feldman, W.C., et al., "Fluxes of Fast and Epithermal Neutrons from Lunar Prospector: Evidence for Water Ice at the Lunar Poles," *Science* **281**, 1496 (1998).
2. *Lunar Prospector Data Archives*, <http://wundow.wustl.edu/lunarp/> (1999).
3. Wittenberg, L.J., J.F. Santarius, and G.L. Kulcinski, "Lunar Source of ^3He for Commercial Fusion Power," *Fusion Technology* **10**, 167 (1986).
4. Wittenberg, L.J., et al., "A Review of ^3He Resources and Acquisition for Use as Fusion Fuel," *Fusion Technology* **21**, 2230 (1992).
5. Swindle, T.D., et al. *Systematic Variations in Solar Wind Fluence with Lunar Location: Implications for Abundances of Solar-Wind-Implanted Volatiles*, in *Lunar and Planetary Sciences Conference XXIII* (1992).
6. Johnson, J.R., T.D. Swindle, and P.G. Lucey, "Estimated Solar Wind-Implanted Helium-3 Distribution on the Moon," *Geophysical Research Letters* **26**, 385 (1999).
7. Daily, W.D., et al., "Ionosphere and Atmosphere of the Moon in the Geomagnetic Tail," *Journal of Geophysical Research* **82**, 5441 (1977).
8. Mutch, T.A., *Geology of the Moon—A Stratigraphic View* (Princeton University Press, Princeton, New Jersey, 1970).
9. *WIND Magnetic Field Investigation Experiment*, <http://lepmpi.gsfc.nasa.gov/mfi/windmfi.html> (1999).
10. Zalewski, M.J. and J.F. Santarius, "Deposition of Solar-Wind Volatiles on the Moon," in preparation.
11. Malecki, M.J., *Investigation of Lunar Pickup-Ion Dynamics*, Progress Report to the National Space Society (1999).
12. Malecki, M.J. and J.F. Santarius, "Dynamics of Lunar Pickup Ions," in preparation.